

Uncertainties from metrology in the integrated luminosity measurement with the updated design of a detector at CEPC

Ivan Smiljanić¹, Ivanka Božović², and Goran Kačarević³

¹ *Vinca Institute of Nuclear Sciences - National Institute of the Republic of Serbia, University of Belgrade, M. Petrovica Alasa 12-14, Belgrade, Serbia*

**E-mail: i.smiljanic@vin.bg.ac.rs*

² *Vinca Institute of Nuclear Sciences - National Institute of the Republic of Serbia, University of Belgrade, M. Petrovica Alasa 12-14, Belgrade, Serbia*

³ *Vinca Institute of Nuclear Sciences - National Institute of the Republic of Serbia, University of Belgrade, M. Petrovica Alasa 12-14, Belgrade, Serbia*

.....
 In order to measure integrated luminosity with a required precision of 10^{-4} at the Z^0 pole, proposed CEPC e^+e^- collider requires a luminometer, a specially designed calorimeter placed in the very forward region to identify Bhabha scattering at low polar angles. Usually, such a device is placed at the outgoing beams, to keep the spatial symmetries of the head-on collisions at accelerators with a non-zero crossing angle. At CEPC it is currently proposed to place the luminometer on the z-axis. We review a feasibility of a measurement of the integrated luminosity at the Z^0 pole with the required precision, concerning the luminometer centered around the z-axis and the post-CDR beam properties.

1 Introduction

In order to achieve precision goals of the electroweak physics program at CEPC at the Z^0 pole, integrated luminosity \mathcal{L} should be known with the total relative uncertainty of order of 10^{-4} [1]. In the CEPC Conceptual Design Report [1], beam properties and detector concept are discussed, with particular emphasis on the machine-detector interface (MDI) and integrated luminosity measurement. The current design of MDI at CEPC has a distinctive feature with respect to the proposal discussed in [1] - the luminometer is proposed to be placed at the z-axis. This is mainly due to the fact that both detector and machine instrumentation occupy low polar angles, with accelerator components being placed in the detector in a conical space inside the opening angle of ~ 118 mrad ($|\cos\theta| \geq 0.993$). Although the impact of metrology on the integrated luminosity measurement at CEPC with the luminometer conventionally placed at the outgoing beams (s-axis) has been discussed in [2], it requires revisiting for the newly proposed geometry, since the integrated luminosity precision critically depends on the luminometer's position, as well as on the event selection.

In this paper, we review the potential impact of locating the luminometer around the z-axis on uncertainties associated with measuring integrated luminosity. These uncertainties stem from mechanical factors like positioning and alignment of the luminometer and the fact that the beam properties are known within some margins. These effects are collectively referred to as metrology. Additionally, we examined the performance of different Bhabha counting methods, including the LEP-style asymmetric counting [3], typically utilized to mitigate systematic biases arising from asymmetries between the left and right detector halves.

The paper is organized as follows: in Section 2 we discuss the current layout of the very forward region of CEPC. In Section 3 we review the impact of detector manufacturing, positioning and alignment (Section 3.1), as well as the impact of uncertainties of the knowledge of the beam properties (asymmetry of beam energies, beam energy spread - BES and beam synchronization) in Section 3.2. The concluding discussion is given in Section 4.

2 Forward region at CEPC

The MDI region of CEPC is proposed to longitudinally cover the area of 12 m with the centrally positioned interaction point (IP). The components of the accelerator (without shielding) will be placed in an 118 mrad cone inside the detector, as illustrated in Fig. 1 [4]. The crossing angle in the horizontal plane between the colliding beams at the IP is 33 mrad. The final focus length of colliding beams is 220 cm [1]. It is proposed that the luminometer

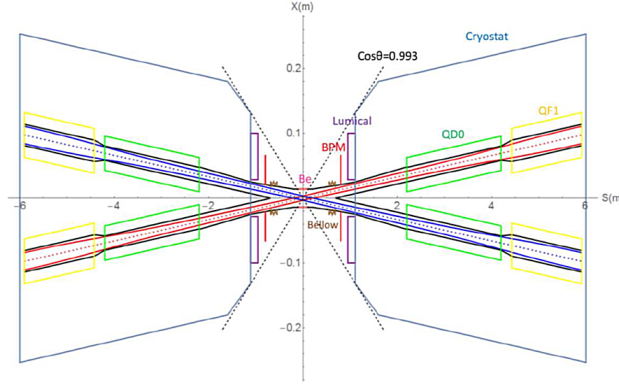


Fig. 1: Schematic view of the MDI region at CEPC.

at CEPC should be placed at 95 cm distance from the interaction point, covering the polar angle region from 30 mrad to 105 mrad, which corresponds to the luminometer aperture of 2.85 cm for the inner and 10.0 cm for the outer radius. The fiducial volume of luminometer should be between 53 mrad and 79 mrad. To prevent the leakage of the electromagnetic showers outside of the luminometer's edges, an iron shielding of 5 mm thickness can be placed around the luminometer. However, this has been done under assumption that the luminometer will be placed around the outgoing beams and it is yet to be proven for the luminometer placed around the z-axis, since the symmetry of signal hits with respect to the detector axis will be lost, as illustrated in Fig. 2 where the hitmap in the first plane of the luminometer is presented.

The choice of technology of the luminometer at CEPC has not been finally determined yet. However, since this study is based on simulation of counting of low-angle Bhabha scattering without any other assumption but the angular acceptance of the luminometer, it is of no relevance for this study. If one would perform a more realistic simulation including detector response to signal and background, at least an energy cut on electron and positron tracks should be required to separate Bhabha events from the background. In such a case, effects like bias and resolution of energy measurement as well as the uncertainties from calibration of the luminometer should be included as additional sources of systematic uncertainty. The same holds if one includes other selection criteria based on polar and azimuthal angles of a Bhabha candidate.

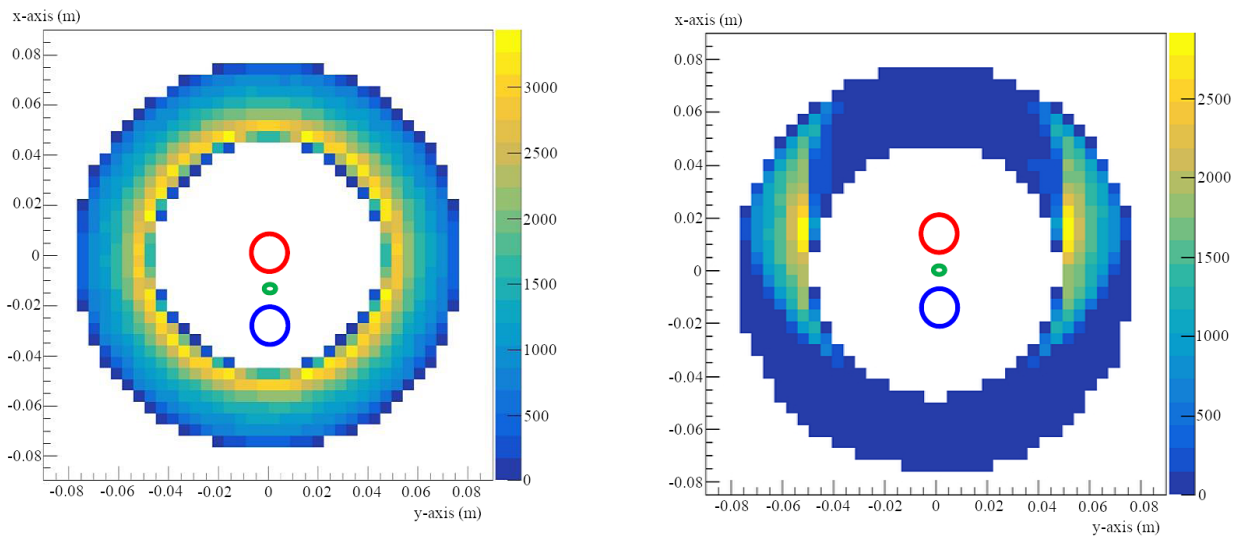


Fig. 2: Hitmap of the first plane of the luminometer placed around the outgoing beam (left) and z-axis (right). Red and blue circles represent the outgoing and incoming beam pipes respectively, and the green circle represents the z-axis.

3 Integrated luminosity measurement and systematic uncertainties

Integrated luminosity measurement is conventionally based on the low angle Bhabha scattering (LABS). It is defined as:

$$\mathcal{L} = \frac{N_{Bh}}{\sigma_{Bh}}, \quad (1)$$

where N_{Bh} is Bhabha count in the certain phase space of parameters and σ_{Bh} is the LABS cross-section. Both Bhabha count and theoretical cross-section at the Z^0 pole should be known at the level of 10^{-4} , in order to know the integrated luminosity with the same precision. The Bhabha cross-section scales with the center-of-mass energy as [5]:

$$\frac{d\sigma}{d\theta} = \frac{2\pi\alpha_{em}^2}{s} \cdot \frac{\sin\theta}{\sin^4(\frac{\theta}{2})} \approx \frac{32\pi\alpha_{em}^2}{s} \cdot \frac{1}{\theta^3}, \quad (2)$$

where α_{em} is the QED constant and θ the polar angle of emitted Bhabha particles. Uncertainty of 10^{-4} of the cross-section implies that the available center-of-mass energy should be known with the absolute uncertainty of $\Delta(\sqrt{s}) \leq 5$ MeV. There is an ongoing work at future Higgs factories [6] to check the feasibility of \sqrt{s} determination using di-muon production reconstructed in the central tracker. However, the required precision seems to be beyond the experimental reach, but, as discussed in [7], many s-channel processes far from the resonance will have the same dependence of the cross-section on the center-of-mass energy,

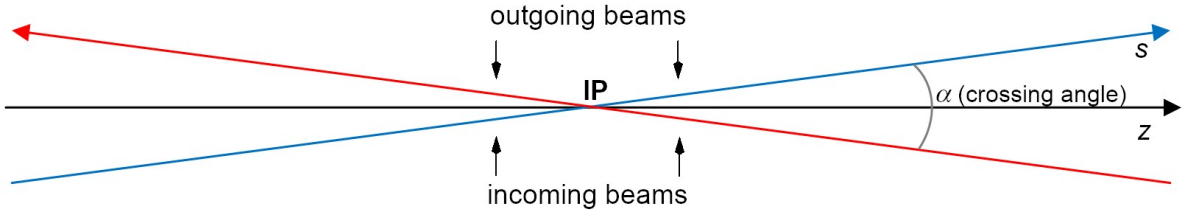


Fig. 3: Illustration of s-axis and z-axis.

leading to effective cancellation of the uncertainties in the cross-section measurements. It is up to each individual cross-section measurement analysis to determine if uncertainty of the integrated luminosity measurement caused by the uncertainty of \sqrt{s} is an issue.

Placement of the luminometer on the z-axis with the CEPC crossing angle of 33 mrad leads to the reduction in Bhabha count for $\sim 70\%$ in comparison to the count with the luminometer placed on the s-axis. Fig. 3 provides an illustrative depiction of the s- and z-axes configurations in collisions with the crossing angle. Since the overall Bhabha count in 16 ab^{-1} of integrated luminosity, which is expected at CEPC at the Z^0 pole, will be of order of 10^{12} for the detector placed on the s-axis, its displacement to the z-axis with the same luminometer apertures will contribute to the relative statistical uncertainty of the count as $1.2 \cdot 10^{-6}$.

Further, feasibility and requirements for 10^{-4} precision of counting at the Z^0 pole will be discussed, considering that the uncertainty of each individual systematic effect contributes to the integrated luminosity at a level of 10^{-4} . In [2], at one side of the luminometer the Bhabhas are counted in the full fiducial volume of the luminometer, while at the other side the inner radial acceptance of the fiducial volume is shrunken by 1 mm. In this study, the outer radial acceptance is also shrunken by 1 mm, as it has been done at OPAL [3], randomly to the left (L) and right (R) sides of the luminometer, on event by event basis. Described way of counting is called asymmetrical throughout the paper. For symmetric event selection the Bhabhas are counted in the full fiducial volumes of the both sides of luminometer. As will be discussed further, different detector positioning (s-axis and z-axis) interfere with a way of counting in a nontrivial way.

3.1 Uncertainties from mechanics and positioning

Systematic uncertainties arising from the detector mechanics and positioning, as well as the uncertainties related to the properties of beams, have been quantified through a

simulation study. We have generated, including the effects of initial (ISR) and final state radiation (FSR), $2 \cdot 10^7$ Bhabha events scattered at low angles at the Z^0 pole, using BHLUMI V4.04 Bhabha event generator [8]. The polar angle range in which the final state particles are generated is from 30 mrad to 100 mrad, to allow events modified by FSR to be detected in the luminometer. In this angular range, the effective Bhabha cross-section is ~ 50 nb.

Considered detector-related uncertainties originating from manufacturing, positioning and alignment of the luminometer are, as in [2]:

- (1) Maximal uncertainty of the luminometer inner aperture, Δr_{in} ,
- (2) RMS of the Gaussian dissipation of the radial shower position measured in the luminometer, with respect to the exact position of the Bhabha hit, σ_r (measured i. e. by placing a tracker plane in front of the luminometer),
- (3) Maximal absolute uncertainty of the distance between left and right sides of the luminometer along the z -axis, Δl , where both halves are shifted equidistantly for $\pm \frac{\Delta l}{2}$ with respect to the interaction point,
- (4) RMS of the Gaussian distribution of luminometer fluctuations with respect to the IP, caused by vibrations and thermal stress, in radial, $\sigma_{x_{IP}}$, and axial direction, $\sigma_{z_{IP}}$.

Figures 4-8 illustrate effects 1-4 respectively, for different ways of counting and different positions of the luminometer placed on the s - and z -axis. Values in histograms shown on Figures 4(a)-8(a) are based on the data from Figures 4(b)-8(b), obtained from the local fit in the region of interest. If the distribution on (b) was not symmetrical for positive and negative variations of the parameter, the more restrictive limit was considered.

Figures 4-8 show that for the detector placed at the z -axis asymmetric counting performs similarly as counting in the full fiducial volume, whereas with the detector placed at the s -axis the difference between the two ways of counting is quite significant. On Figure 4, which illustrates the impact of Δr_{in} , it can be seen that the counting uncertainties with the detector placed at the z -axis are similar to uncertainties when counting in the full fiducial volume with the detector placed at the s -axis. For σ_r and $\sigma_{z_{IP}}$, the requirements are slightly more relaxed for the luminometer placed at the z -axis than with the asymmetric counting with the luminometer placed at the s -axis, as shown in Figures 5 and 8, whether for $\sigma_{x_{IP}}$ it's the other way around. For Δl , the uncertainties are the same for both positions of the luminometer and for both ways of counting, as illustrated in Figure 6. However, one has to keep in mind that the results shown in this paper are based on distributions of mean values, each obtained from the simulated signal sample of $2 \cdot 10^7$ events, with intrinsic relative statistical uncertainty of $\sim 2 \cdot 10^{-4}$. Therefore, the extracted precision limits rather reflect the order of magnitude

required to control certain mechanical or beam properties at the level of 10^{-4} than the exact values of detector or beam parameters.

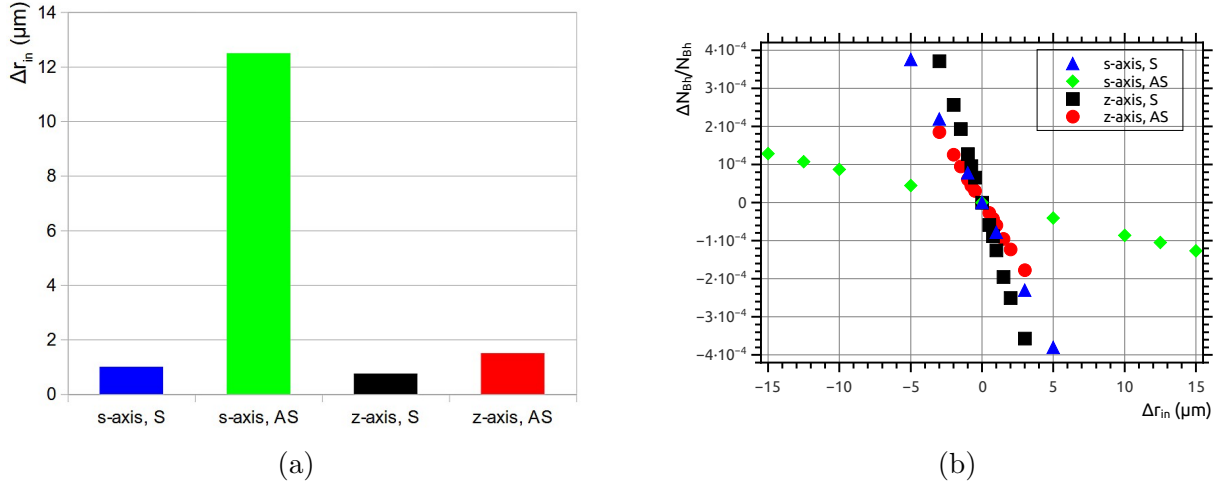


Fig. 4: (a) Variations of the inner aperture (counting volume), Δr_{in} , for two different ways of counting: in the full fiducial volume (S) and the LEP-style (AS), for detector placed on the s- and z-axis; (b) Count uncertainty as a function of Δr_{in} for two different ways of counting (S and AS), with the detector placed at the s- and z-axis.

3.2 Beam related uncertainties

Several systematic uncertainties may arise from uncertainties of the properties of the beams and their delivery to the interaction point. The list of CEPC beam parameters addressed in this study is given in Table 1 [9].

Table 1: CEPC TDR beam parameters at the Z^0 pole.

parameter	Z^0 pole
Half crossing angle at IP (mrad)	16.5
Energy (GeV)	45.5
Bunch population (10^{11})	1.4
Bunch length (natural/total) (mm)	2.7/10.6
Beam size at IP σ_x/σ_y ($\mu\text{m}/\text{nm}$)	6/35
Energy spread (natural) (%)	0.04
Luminosity per IP ($10^{34} \text{ cm}^{-2}\text{s}^{-1}$)	115

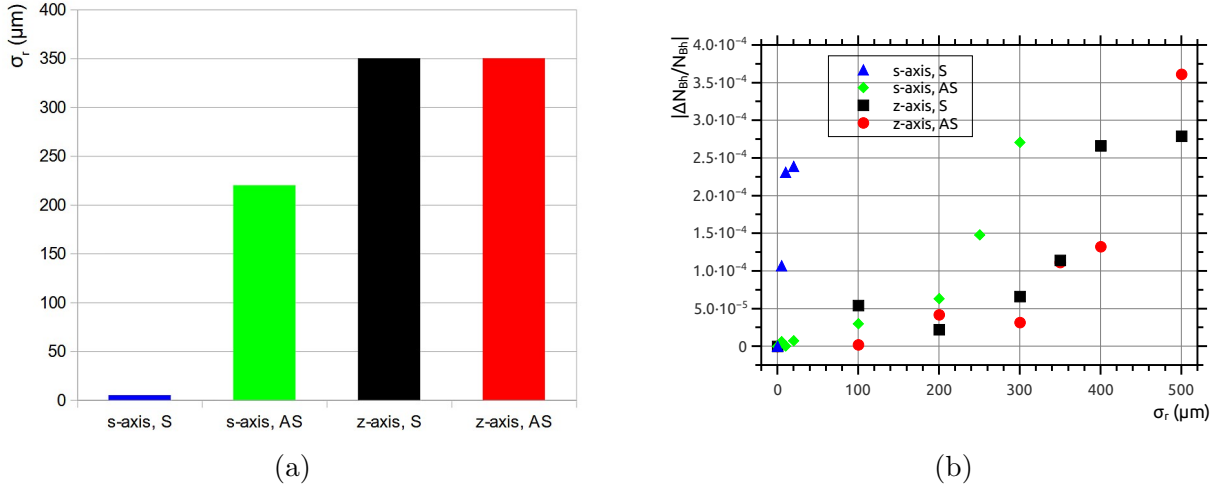


Fig. 5: (a) A comparison of results between the luminometer placed at the s-axis and luminometer placed at the z-axis for the RMS of the Gaussian spread of measured radial shower position with respect to the true one, σ_r . (b) Count uncertainty as a function of σ_r for two different ways of counting (S and AS), with the detector placed at the s- and z-axis.

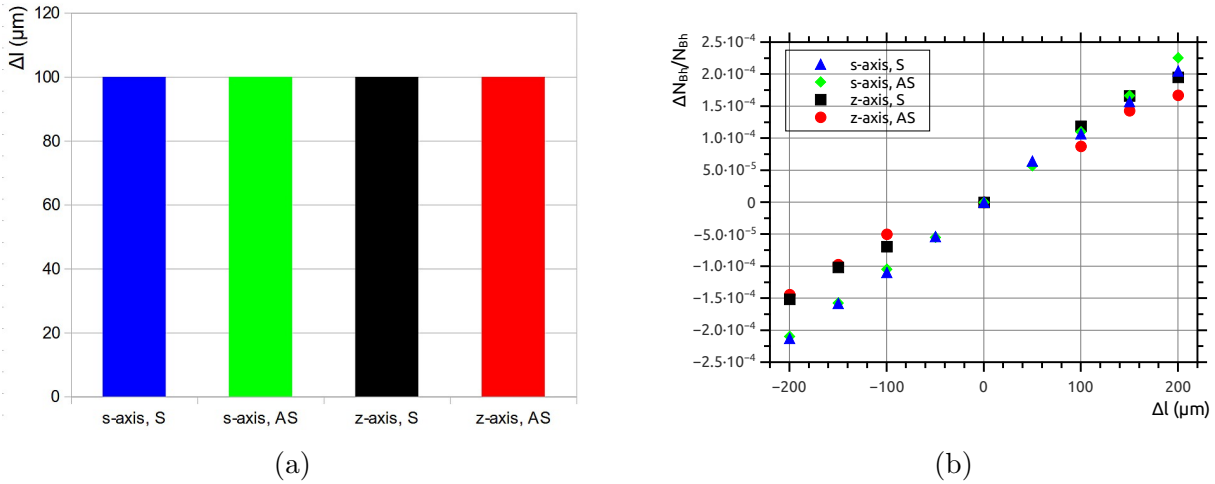


Fig. 6: (a) A comparison of results between the luminometer placed at the s-axis and luminometer placed at the z-axis for maximal absolute uncertainty, Δl , of the longitudinal distance between left and right luminometer sides; (b) Count uncertainty as a function of Δl for two different ways of counting (S and AS), with the detector placed at the s- and z-axis.

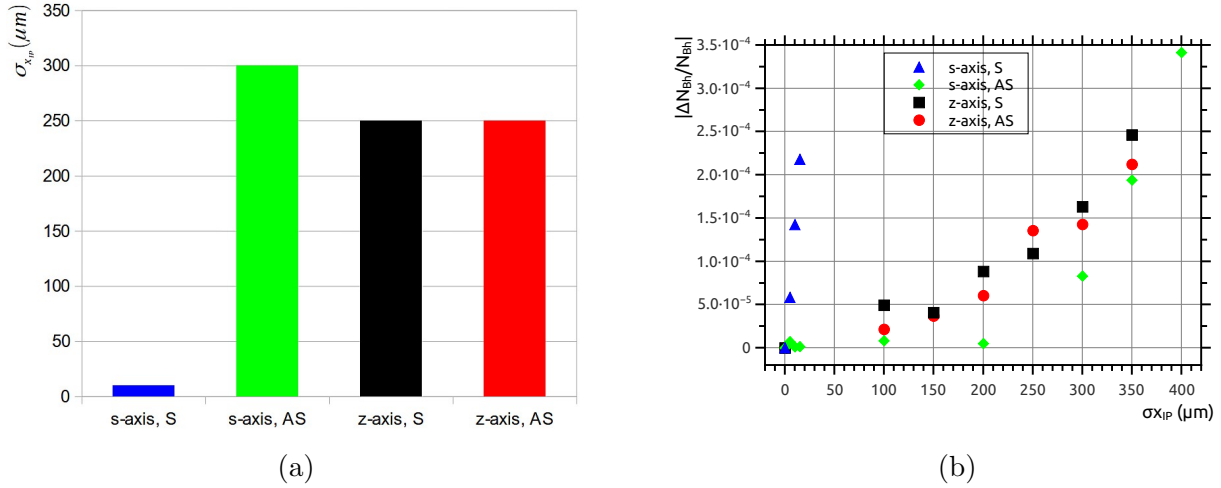


Fig. 7: (a) A comparison of results between the luminometer placed at the s-axis and luminometer placed at the z-axis against the RMS of a Gaussian distribution of radial fluctuations of the luminometer position with respect to the IP, $\sigma_{x_{IP}}$; (b) Count uncertainty as a function of $\sigma_{x_{IP}}$ for two different ways of counting (S and AS), with the detector placed at the s- and z-axis.

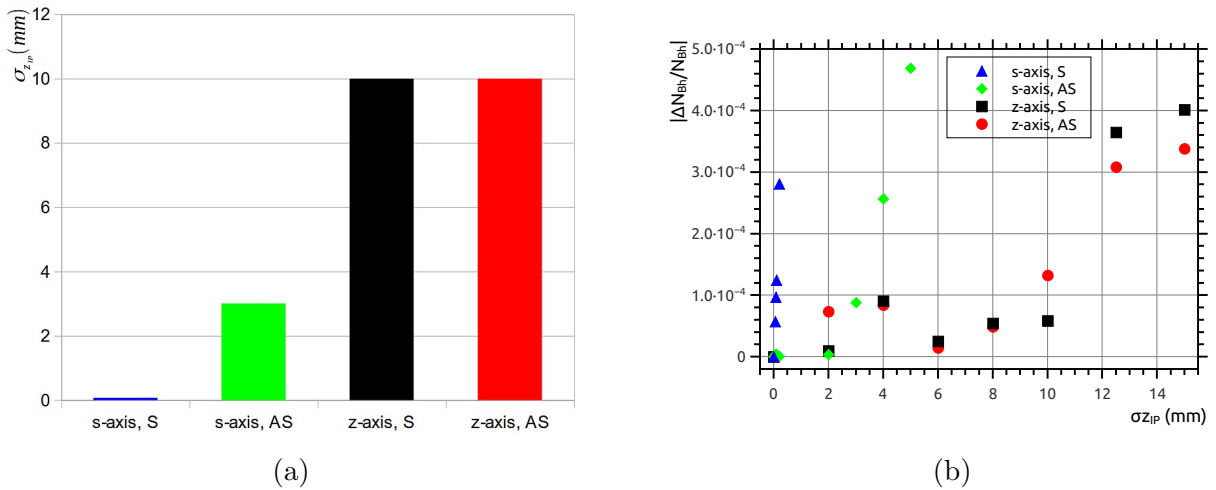


Fig. 8: (a) A comparison of results between the luminometer placed at the s-axis and luminometer placed at the z-axis against the RMS of the Gaussian distribution of axial fluctuations of the luminometer position with respect to the IP, $\sigma_{z_{IP}}$; (b) Count uncertainty as a function of $\sigma_{z_{IP}}$ for two different ways of counting (S and AS), with the detector placed at the s- and z-axis.

Here we consider, again similarly to [2]:

- (1) maximal permanent bias (ΔE) of a single beam energy with respect to the other beam, resulting in a longitudinal boost of the incoming e^+e^- system with respect to the laboratory frame, and consequently, boost of the Bhabha center-of-mass system,
- (2) maximal RMS of the Gaussian distribution of the beam energy spread ($\sigma_{E_{BS}}$), responsible for longitudinal boost on event-by-event basis, leading to the overall count loss of order of 10^{-4} ,
- (3) maximal radial (Δx_{IP}^{BS}) and axial (Δz_{IP}^{SY}) IP position displacements with respect to the luminometer arms, caused by the finite beam sizes (former) and beam synchronization (latter),
- (4) maximal time shift in beam synchronization ($\Delta\tau_{SY}$), determined from Δz_{IP}^{SY} , which may cause the IP longitudinal displacement Δz_{IP}^{SY} .

In the same manner as in the previous chapter, results for effects 1-4 are illustrated on Figures 9-12 and the upper limits, together with the upper limits of mechanical parameters from Section 3.1, are summarized in Table 2. Each effect is considered to individually contribute to the the relative uncertainty of the integrated luminosity as $1 \cdot 10^{-4}$.

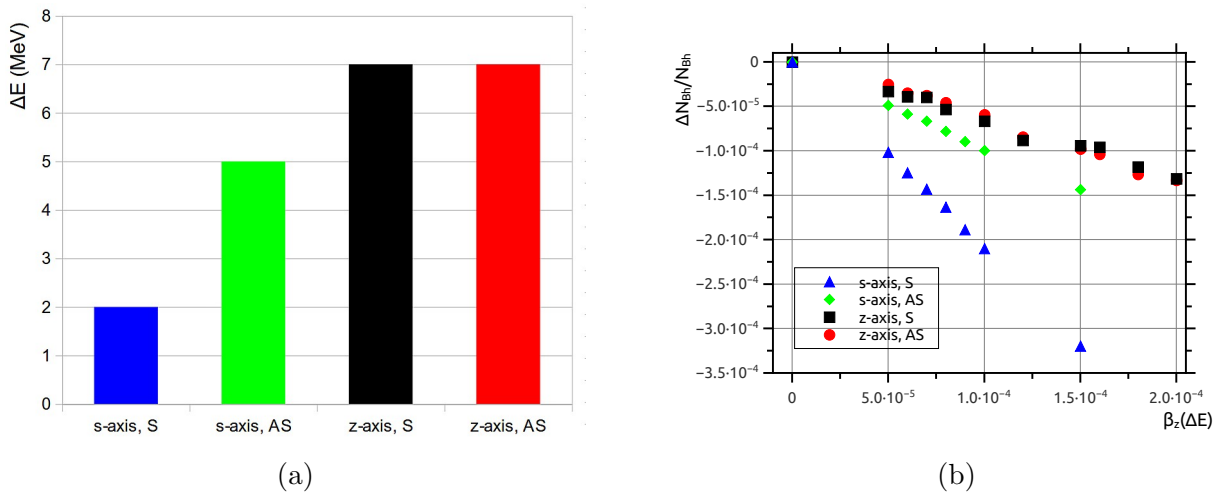


Fig. 9: (a) A comparison of results between the luminometer placed at the s-axis and luminometer placed at the z-axis for maximal bias of energy of one beam with respect to the other, ΔE ; (b) Loss of the Bhabha count in the luminometer due to the longitudinal boost of the center-of-mass frame, $\beta_z(\Delta E)$, for two different ways of counting (S and AS), with the detector placed at the s- and z-axis.

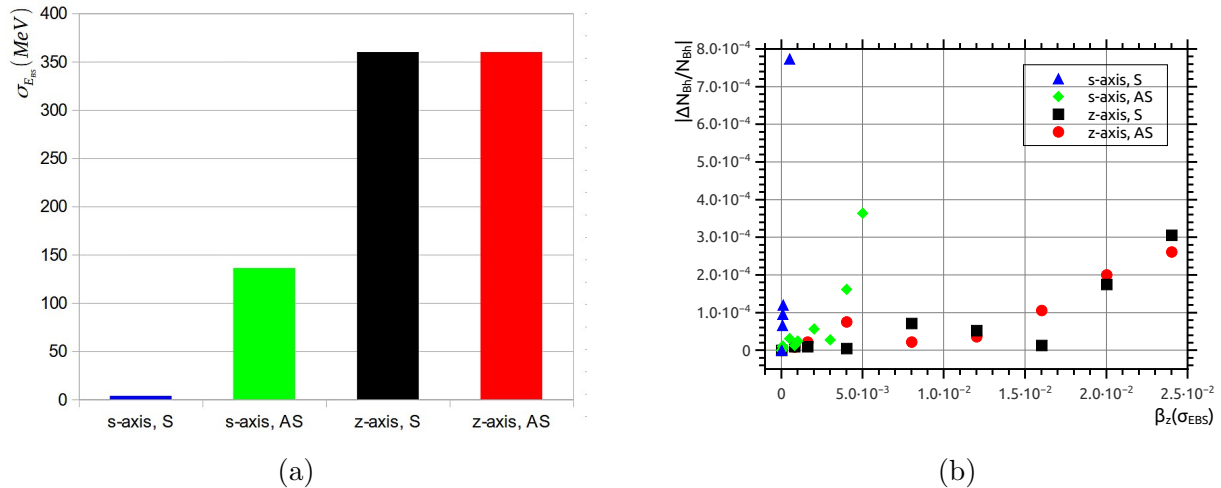


Fig. 10: (a) A comparison of results between the luminometer placed at the s-axis and luminometer placed at the z-axis for maximal RMS of the BES Gaussian distribution, corresponding to the relative systematic uncertainty of \mathcal{L} of 10^{-4} , $\sigma_{E_{BS}}$; (b) Loss of the Bhabha count in the luminometer due to longitudinal boost of the Bhabha center-of-mass frame caused by BES, $\beta_z(\sigma_{E_{BS}})$, for two different ways of counting (S and AS), with the detector placed at the s- and z-axis.

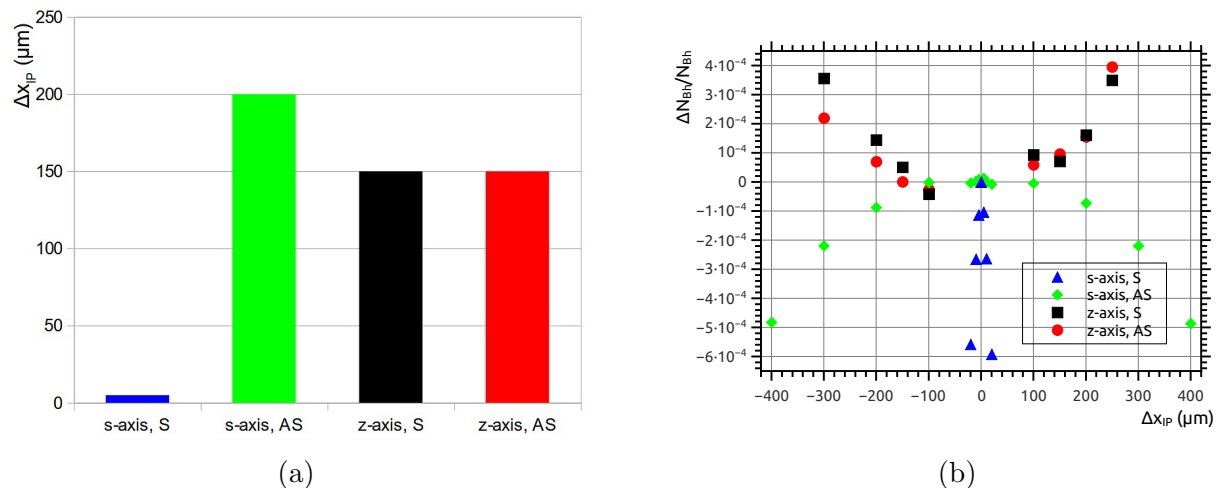
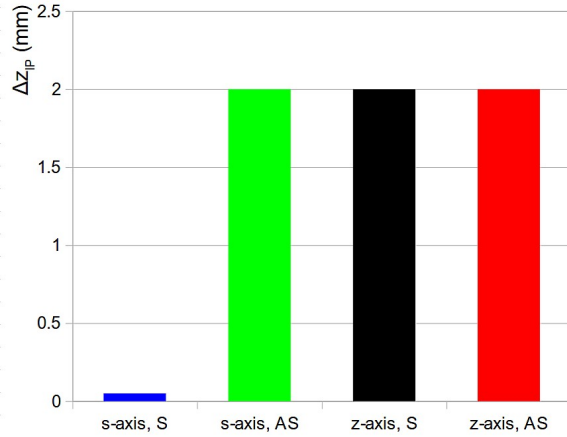
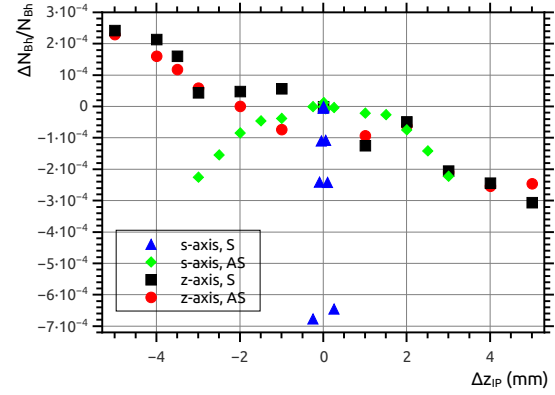


Fig. 11: (a) A comparison of results between the luminometer placed at the s-axis and luminometer placed at the z-axis for maximal radial IP position displacement with respect to the luminometer (Δx_{IP}^{BS}); (b) Count uncertainty as a function of Δx_{IP}^{BS} for two different ways of counting (S and AS), with the detector placed at the s- and z-axis.



(a)



(b)

Fig. 12: (a) A comparison of results between the luminometer placed at the s-axis and luminometer placed at the z-axis for maximal axial IP position displacements with respect to the luminometer (Δz_{IP}^{BS}); (b) Count uncertainty as a function of Δz_{IP}^{BS} for two different ways of counting (S and AS), with the detector placed at the s- and z-axis.

Table 2: Minimal absolute precision of luminometer mechanical parameters and beam parameters, each contributing as 10^{-4} to the relative uncertainty of \mathcal{L} at the Z^0 pole. The average net center-of-mass energy uncertainty ΔE_{CM} limit is derived by error propagation from the Bhabha cross-section dependence on the center-of-mass energy.

parameter	s-axis, symm.	s-axis, asymm.	z-axis, symm.	z-axis, asymm.
Δr_{in} (μm)	1	12	0.8	1.5
σ_r (μm)	5	220	350	350
Δl (μm)	100	100	100	100
$\sigma_{x_{IP}}$ (μm)	10	300	250	250
$\sigma_{z_{IP}}$ (mm)	0.08	3	10	10
ΔE_{CM} (MeV)	5	5	5	5
ΔE (MeV)	2	5	7	7
$\sigma_{E_{BS}}$ (MeV)	4	140	360	360
Δx_{IP}^{BS} (μm)	5	200	150	150
Δz_{IP}^{SY} (mm)	0.05	2	2	2
$\Delta\tau$ (ps)	0.08	3	3	3

As can be seen from Table 2, mechanical precision of the luminometer's inner aperture seems to be the major challenge, since the Bhabha cross-section is scaling with the polar angle as $\sigma \sim 1/\theta^3$. The longitudinal boost of the Bhabha center-of-mass frame with respect to the laboratory frame, β_z , may be caused by any difference in beam energies, δE ($\beta_z = 2 \cdot \delta E / \sqrt{s}$), in the form of bias of one beam with respect to the other, ΔE , or as a random asymmetry caused by the beam energy spread or by other radiative losses. All limits of parameters given in Table 2 are derived from distributions of mean values in Figures 4(b) - 12(b), without considering statistical uncertainties from the limited size of the simulated samples. From Table 2 it can be seen that in terms of the beam-related parameters precision, displacement of the luminometer from the s-axis to the z-axis will not impact the luminosity precision significantly, while some dependencies between observables, especially Δx_{IP}^{BS} , Δz_{IP}^{SY} (Figures 11 and 12) will be modified due to loss of spacial symmetries of Bhabha events.

4 Conclusion

Although the method of integrated luminosity has been studied in a great detail at LEP ([10], [11]), for each newly proposed e^+e^- collider it is necessary to quantify the achievable luminosity precision, in particular at the Z^0 resonance. Here it is done for CEPC, taking into consideration the mechanical and beam-related requirements at the Z^0 pole, with the

luminometer placed on the z -axis. It is the first attempt to quantify systematic effects rising from metrology with the luminometer displaced from the the outgoing beams, where it is conventionally positioned at colliders with a crossing angle.

Control of the luminometer inner radius at the micrometer level at the Z^0 pole seems to be the most demanding requirement for the detector manufacturing, regardless of the luminometer's positioning (on the s -axis or on the z -axis). Any eventual change in the luminometer design towards smaller polar angle coverage will require control of the luminometer inner radius even below micrometer precision, according to the dependence of the Bhabha cross-section on the polar angles of the scattered particles. However, it is important to note that these results are obtained under assumption that the change of the luminometer's inner radius corresponds to exactly the same change of the inner radius of the luminometer's fiducial volume, which needs to be approved. Also, control of the asymmetrical bias in beam energies might be challenging, while the beam energy spread can be relaxed significantly beyond the current RMS of 18 MeV at the Z^0 pole.

From the point of view of experimental input for the Bhabha cross-section calculations, center-of-mass energy should be known at the 10^{-4} level, which requires further studies in terms of feasibility of such a precision. This might be an issue for the cross-section measurements on the slope of a production threshold.

Although the simulated Bhabha samples are relatively small to be exact on boundaries of the considered systematics, distribution of central values presented in this study confirms that no effect seems to be more critical for precision measurement of the integrated luminosity if the luminometer is placed around the z -axis than if it is placed around the outgoing beams. The LEP-style asymmetric counting, however, will not be effective for the luminometer placed on the z -axis to cope with the effects arising from the left-right asymmetry.

Complex metrology, together with the beam-related interactions affecting the Bhabha final state at small polar angles [12] may call for consideration of an alternative or a complementary central process for the integrated luminosity measurement, like di-photon or di-muon production (under the assumption that this process at the Z^0 pole energy doesn't receive relevant contributions from the processes beyond the Standard Model), with hopefully less complex systematic effects subjected to further studies [13]. In addition, studies presented here should be complemented with a full simulation study of systematic effects arising from the detector design, technology and performance in the presence of realistic backgrounds.

Acknowledgment

This research was funded by the Ministry of Education, Science and Technological Development of the Republic of Serbia and by the Science Fund of the Republic of Serbia through the Grant No. 7699827, IDEJE HIGHTONE-P.

References

- [1] The CEPC Study Group, CEPC Conceptual Design Report: Volume 2 - Physics & Detector [arXiv:1811.10545 [hep-ex]] (2018). <https://doi.org/10.48550/arXiv.1811.10545>
- [2] I. Smiljanic et al., JINST **17** P09014 (2022). [10.1088/1748-0221/17/09/P09014](https://doi.org/10.1088/1748-0221/17/09/P09014)
- [3] G. Abbiendi et al. [OPAL Collaboration], Eur.Phys.J.C **14**, 373–425 (2000). <https://doi.org/10.1007/s100520000353>
- [4] S. Hou, *Updates of the CEPC LumiCal Design*, talk given at the Joint Workshop of the CEPC Physics, Software and New Detector Concept in 2022, 2022.
- [5] H Abramowicz et al. [FCAL Collaboration], JINST **5** P12002 (2010). [10.1088/1748-0221/5/12/P12002](https://doi.org/10.1088/1748-0221/5/12/P12002)
- [6] G. Wilson, *Center-of-mass energy determination using dimuon events at ILC*, talk given at ILC Workshop on Potential Experiments (ILCX2021) (2021). https://agenda.linearcollider.org/event/9211/contributions/49276/attachments/37409/58737/ILCX_GWW_V3.pdf
- [7] A. Stahl, LC-DET-2005-004 (2005). <https://bib-pubdb1.desy.de/record/587787/files/LC-DET-2005-004.pdf>
- [8] S. Jadach et al., Comput.Phys.Commun. **102**, 229–251 (1997). [https://doi.org/10.1016/S0010-4655\(96\)00156-7](https://doi.org/10.1016/S0010-4655(96)00156-7)
- [9] J. Gao, *CEPC Accelerator General Status Overview*, talk given at The 2023 International Workshop on CEPC (EU Edition) (2023). https://indico.ph.ed.ac.uk/event/259/contributions/2466/attachments/1305/1959/CEPC_Accelerator_General_Status_Overview-v1.pdf
- [10] B. Pietrzyk, LAPP-EXP-94.18 (1994). https://inis.iaea.org/collection/NCLCollectionStore/_Public/26/072/26072195.pdf
- [11] I.C. Brock et al. Nucl. Instrum. Methods Phys. Res. A 381 **2-3**, 236-266 (1996). [https://doi.org/10.1016/S0168-9002\(96\)00734-6](https://doi.org/10.1016/S0168-9002(96)00734-6)
- [12] G. Voutsinas, E. Perez, M. Dam et al. J.High Energ.Phys. **225** (2019). [https://doi.org/10.1007/JHEP10\(2019\)225](https://doi.org/10.1007/JHEP10(2019)225)
- [13] J. de Blas et al. *Focus topics for the ECFA study on Higgs / Top / EW factories*, (2024)[arXiv:2401.07564 [hep-ph]]. <https://doi.org/10.48550/arXiv.2401.07564>